THE JOURNAL OF BIOLOGICAL CHEMISTRY VOL. 291, NO. 33, pp. 17332–17344, August 12, 2016

Structure and Function of Cross-class Complexes of G Protein-coupled Secretin and Angiotensin 1a Receptors*

Received for publication, April 2, 2016, and in revised form, June 16, 2016 Published, JBC Papers in Press, June 21, 2016, DOI 10.1074/jbc.M116.730754

Kaleeckal G. Harikumar[‡], Mary Lou Augustine[‡], Leo T. O. Lee[§1], Billy K. C. Chow[¶2], and Laurence J. Miller[‡3]

From the [‡]Department of Molecular Pharmacology and Experimental Therapeutics, Mayo Clinic, Scottsdale, Arizona 85259, the [§]Centre of Reproduction, Development and Aging, University of Macau, Taipa, Macau, and the [¶]School of Biological Sciences, The University of Hong Kong, Pokfulam Road, Hong Kong

Complexes of secretin (SecR) and angiotensin 1a (Atr1a) receptors have been proposed to be functionally important in osmoregulation, providing an explanation for overlapping and interdependent functions of hormones that bind and activate different classes of GPCRs. However, the nature of these cross-class complexes has not been well characterized and their signaling properties have not been systematically explored. We now use competitive inhibition of receptor bioluminescence resonance energy transfer and bimolecular fluorescence complementation to establish the dominant functionally important state as a symmetrical homodimeric form of SecR decorated by monomeric Atr1a, interacting through lipid-exposed faces of Atr1a TM1 and TM4. Conditions increasing prevalence of this complex exhibited negative allosteric modulatory impact on secretin-stimulated cAMP responses at SecR. In contrast, activating Atr1a with full agonist in such a complex exhibited a positive allosteric modulatory impact on the same signaling event. This modulation was functionally biased, with secretin-stimulated calcium responses unaffected, whereas angiotensin-stimulated calcium responses through the complex were reduced or absent. Further supporting this interpretation, Atr1a with mutations of lipid-exposed faces of TM1 and TM4 that did not affect its ability to bind or signal, could be expressed in the same cell as SecR, yet not exhibit either the negative or positive allosteric impact on cAMP observed with the inactive or activated states of wild type Atr1a on function, and not interfere with angiotensin-stimulated calcium responses like complexes with Atr1a. This may provide a more selective means of exploring the physiologic functional impact of this cross-class receptor complex without interfering with the function of either component receptor.

The association of proteins within the plasma membrane is a well recognized molecular mechanism for regulation of signaling. Receptor-tyrosine kinases form dimeric complexes that are responsible for cross-phosphorylation and activation (1). Although guanine nucleotide-binding protein (G protein)-coupled receptors (GPCRs)[4] can be shown to function as monomers (2), these have also been shown to associate with themselves or with each other to form oligomeric complexes (3). Such complexes follow themes characteristic of each of the main groups (families) of GPCRs, with the class C GPCRs forming obligate dimeric complexes that can even be disulfide bonded to each other for stability (4), the class A GPCRs described as ranging from working as monomers to transient dimers or even higher order complexes (5), and the class B GPCRs described as somewhere in between, forming relatively stable dimeric complexes (6). It has been quite rare to recognize cross-class GPCR complexes that have physiologic functional significance (7).

The association between the class A type 1a angiotensin receptor (Atr1a) and the class B secretin receptor (SecR) represents such a complex (8). Both of these receptors and their natural hormonal agonists are present in brain osmoregulatory centers in the circumventricular organ and the hypothalamic paraventricular nucleus (9, 10) providing the opportunity for meaningful interaction. Both signaling systems have been shown to regulate drinking behavior *in vivo* (9–11). Angiotensin-II (ANG-II) and secretin are both elevated in the periphery and in the central nervous system in response to hyperosmolality, with this leading to vasopressin release and increased water intake (9, 11). These effects have also been shown to be interdependent, with drinking responses to ANG-II disrupted in secretin peptide and receptor knock-out animals (9, 12).

It has been suggested that the overlapping and interdependent osmoregulatory functions of these two hormones could be explained by a direct interaction between their receptors (9, 10, 12). The SecR-Atr1a hetero-receptor complex was shown to exist *in vitro*, when both receptors were co-expressed on a model cell, with this complex able to modify some of the signaling responses to their natural agonist ligands (8), recapitulating the events observed *in vivo* in intact mice (8). In our recent work, we showed that peptides representing key transmembrane segments of both of these receptors were able to affect these hetero-receptor complexes and their function (8). This

* This work was supported, in whole or in part, by National Institutes of Health Grant DK046577 (to L. J. M.) and the Mayo Clinic (to L. J. M.). The authors declare that they have no conflict of interest with the content of this article. The content is solely the responsibility of the authors and does not necessarily represent the official views of the National Institutes of Health.

[1] Supported by Fundo para o Desenvolvimento das Ciências e da Tecnologia Grant FDCT101/2015/A3, Macao.

[2] Supported by Hong Kong Government RGC Grants CRFHKU6/CRF/11G, HKU 764812M, and HKU 765011M.

[3] To whom correspondence should be addressed: 13400 East Shea Blvd., Scottsdale, AZ 85259. Tel.: 480-301-4217; Fax: 480-301-8387; E-mail: miller@mayo.edu.

[4] The abbreviations used are: GPCR, G protein-coupled receptor; Atr1a, angiotensin type 1a receptor; BRET, bioluminescence resonance energy transfer; CCK, cholecystokinin; CCK1R, type 1 CCK receptor; CCK2R, type 2 CCK receptor; Rlu, *Renilla* luciferase; SII, [Sar[1],Ile[4],Ile[8]]angiotensin-II; SecR, secretin receptor; YC, YFP(159–238); YN, YFP(1–158); BiFC, bimolecular fluorescence complementation; TM, transmembrane.

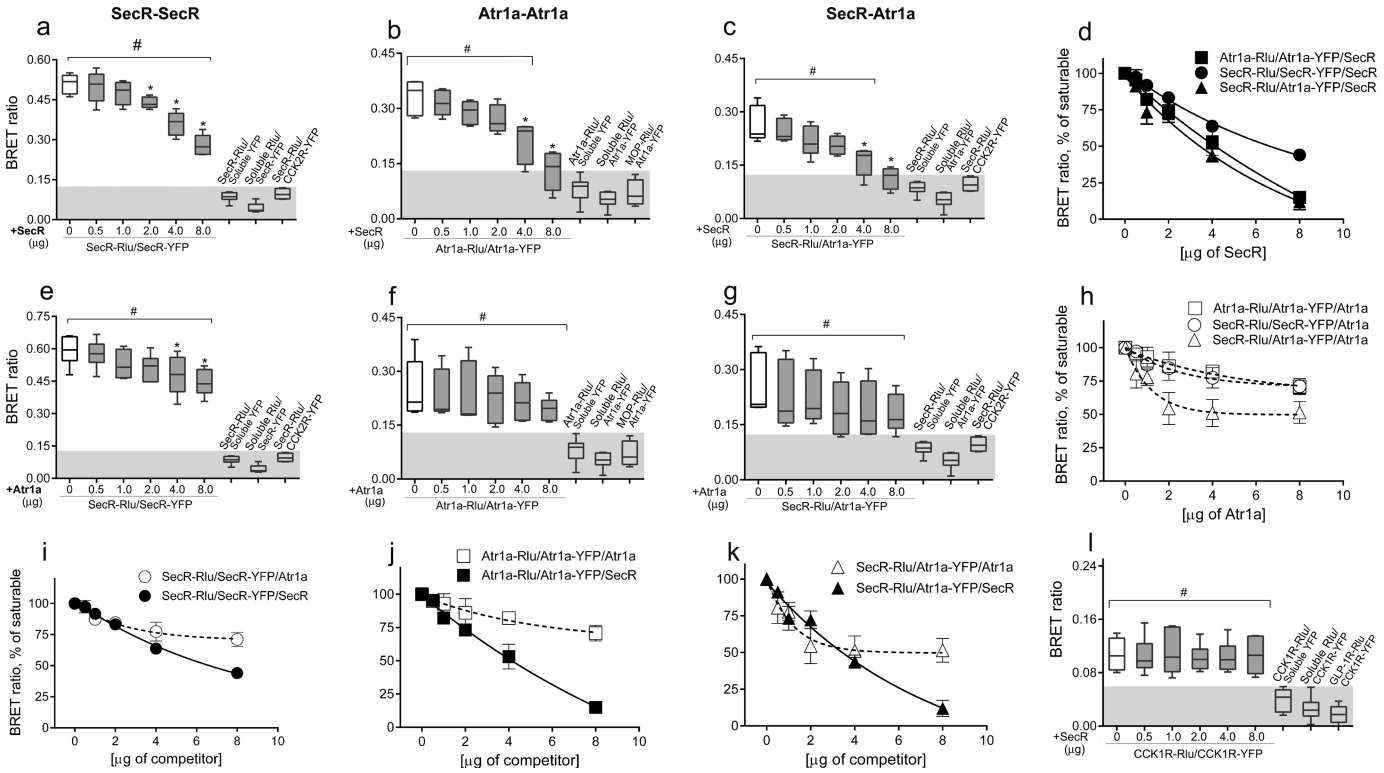

FIGURE 1. **Wild type receptor BRET studies.** Shown are results of static BRET studies involving resonance transfer between SecR-SecR (*panels a*, *e*, and *i*), Atr1a-Atr1a (*panels b*, *f*, and *j*), and SecR-Atr1a (*panels c*, *g*, and *k*), using 1 μg of donor and 1 μg of acceptor construct. The ability of unlabeled receptor to compete for this signal is also studied, with the results graphed as percentages of the saturable BRET signal (*panels d* and *h–k*). The *shaded area* represents the nonspecific BRET signal generated between the Rlu-tagged receptor or interest and a YFP-tagged receptor known not to associate with the receptor of interest. All of the experimental and control receptors were shown to be expressed at similar levels, based on their YFP signals. Another control was the test of the ability of SecR to disrupt a BRET signal from an unrelated receptor (CCK1R, expressed at ~85% the level of the other receptors) (*panel l*). Data represent mean ± S.E. of 4–6 independent experiments performed in duplicate. * indicates BRET signals significantly different from control, $p < 0.05$; # indicates BRET signals significantly above background, $p < 0.05$.

provided the basis for proposing that the two receptors associate through lipid-facing surfaces of their intact helical bundles. The importance of the transmembrane regions was also supported by demonstrating that the cross-class complex continued to form in the presence of amino-terminal and carboxyl-terminal tail truncations of the component receptors (13).

However, the nature of the cross-class GPCR hetero-complexes has not previously been well characterized. In the current work, we attempt to gain new insights into the nature of the SecR-Atr1a complexes and the molecular basis for the impact of these structures on function. We also work to develop a variant of one of these component receptors that can ultimately be utilized to disrupt such complexes without interfering with the function of the separate receptors.

Results

Both the secretin receptor (SecR) (14) and the type 1a angiotensin receptor (Atr1a) (15) have been reported to form homo-receptor complexes within the plasma membrane of receptor-expressing cells. Additionally, we have reported that the class B SecR can form cross-class hetero-receptor complexes with the class A Atr1a when they are both expressed on the same cell (8), and that such complexes appear to play a key role in mediating water drinking behavior in response to hyperosmotic stress (9). We also demonstrated that delivery of synthetic transmembrane peptides corresponding to TM1 and TM4 segments of Atr1a were able to disrupt these complexes based on hetero-receptor BRET studies, and that these peptides affected hyperosmolality-induced drinking behavior *in vivo* when injected into mice (8). When these TM segment peptides were modified to change the character of their hydrophobic face, they no longer disrupted the hetero-receptor BRET signal and had no effect on drinking behavior *in vivo* (8). The other Atr1a TM segment peptides did not have any effect on the hetero-receptor BRET signal (8). This was interpreted as supporting the hypothesis that SecR-Atr1a complexes are important to regulate water homeostasis and drinking behavior, and supported a level of selectivity in the formation of these complexes. However, the specific nature of these complexes was not established and the lipid-exposed faces of Atr1a TM1 and TM4 were not mutated in the intact receptor as possible confirmation that the TM segment peptides corresponded to their site of action in a more physiological system. In the current study, we have further explored the molecular architecture of this hetero-receptor complex and its functional effect on different signaling cascades.

Fig. 1 illustrates the results of homo- and hetero-receptor BRET studies for SecR and Atr1a, confirming previous reports of significant BRET signals for all three types of complexes (two homo-receptor complexes and one hetero-receptor complex), as well as providing unique new insights into the stability of the

complexes formed. For this effort, 1 μg of donor construct and 1 μg of acceptor construct was utilized in the absence or presence of competing untagged SecR or Atr1a constructs. These conditions yielded 95,000 ± 12,000 SecR sites/cell and 90,000 ± 6,000 Atr1a sites/cell, with a variation of expression of these constructs across all conditions, based on YFP fluorescence, of less than 5%. Nonspecific BRET signals were established by the co-expression of the tagged receptor along with the complementary donor or acceptor as soluble construct. Competing untagged SecR disrupted all of the types of receptor BRET signals to a greater degree than did Atr1a, with the latter only partially reducing these signals. This was true of both homo-receptor complexes, including the complex composed of only the opposite receptor, as well as the hetero-receptor complex. In both conditions, the SecR-Atr1a hetero-receptor complex was more easily inhibited than the homo-receptor complexes. The SecR homo-receptor complex appeared to be the most stable of the three complexes, based on its refractoriness to disruption with untagged SecR. An important control was to test the ability of untagged SecR to disrupt the homo-receptor BRET signal for CCK1R, known not to interact with SecR (16). Indeed, SecR had no effect on that BRET signal (Fig. 1*l*).

Presumably, the observed partial inhibition of the receptor BRET signals with untagged Atr1a reflected association of that receptor with both of the other tagged receptors, thereby depleting the system of available donor and/or acceptor. We probably did not achieve a high enough concentration of the untagged Atr1a in these experiments to fully disrupt even the Atr1a homo-receptor complexes. As a class A GPCR, Atr1a likely associates with itself through multiple interfaces making such competition less efficient, and perhaps requiring a higher stoichiometric ratio of competitor to be effective. In contrast, untagged SecR more completely inhibited the receptor BRET signals, likely reflecting a single dominant interface for the SecR homodimer and possibly reflecting the importance of that structure as the base for the hetero-receptor complex.

To explore this further, we utilized bimolecular fluorescence complementation (BiFC). Fig. 2 shows the key studies to validate this approach, as well as the results documenting the ability of Atr1a to associate with an intact SecR homodimeric complex. All of these constructs bound their respective natural agonist ligand with high affinities that were not different from each other (mean ± S.E. of $p\mathrm{IC}_{50}$ values: Atr1a constructs 8.0 ± 0.1; SecR constructs 8.2 ± 0.1), and exhibited full cAMP responses to natural agonist, with $p\mathrm{EC}_{50}$ values that were not different from each other (mean ± S.E. of values from 4 to 7 independent experiments: Atr1a, 9.4 ± 0.2; Atr1a-Rlu, 9.4 ± 0.2; Atr1a-YFP, 9.4 ± 0.2; Atr1a-YN, 9.1 ± 0.2; Atr1a-YC, 9.7 ± 0.1; SecR, 10.7 ± 0.2; SecR-Rlu, 10.1 ± 0.2; SecR-YFP, 10.3 ± 0.1; SecR-YN, 9.8 ± 0.2; SecR-YC, 10.0 ± 0.1). Shown in Fig. 2*a* are the fluorescence emission spectra for both receptors tagged with an intact YFP construct, as well as the non-fluorescent halves of YFP that can associate in a receptor homodimeric complex to yield a fluorescent YFP. In every situation, the fluorescence could be observed at the cell surface with anisotropy values in the 0.2–0.3 range (Fig. 2, *c* and *b*, respectively). This was included, because the probability of resonance transfer is dependent not only on distance between donor and acceptor, but also on their relative orientation (17), with these values assuring overlapping electronic transitions that minimize possible errors in distance measurements (18). As shown earlier, SecR only forms a homodimeric complex along its lipid-facing surface of TM4 (19), and not higher order complexes (20), as demonstrated by the absence of a significant BRET signal between the BiFC dimer and another complementary tagged SecR (Fig. 2*d*). In contrast, adding the complementary tagged Atr1a to the SecR BiFC dimer did yield a significant BRET signal. This was also confirmed by the saturation BRET data shown (Fig. 2*e*). In contrast to this, complementary tagged SecR did not add to the Atr1a BiFC dimer to yield a significant BRET signal. This may reflect the distances or geometry of such a complex or the possibility that it does not exist as a prominent complex. These data support the presence of monomeric and homodimeric Atr1a, homodimeric SecR, and a prominent complex representing homodimeric SecR with associated monomeric Atr1a. Other complexes are less prominent, but may well exist transiently.

We attempted to extend the insights from the previous TM segment mixing studies to try to confirm the implications of those studies, and to learn more about these complexes. As previously reported, SecR TM4 peptide was the only TM segment peptide from that receptor to disrupt the SecR homo-receptor BRET signal (19, 21) and the impact of the lipid face of that receptor segment was confirmed with an intact SecR mutant (19). Atr1a TM4 peptide was the only TM segment peptide from that receptor to disrupt the Atr1a homo-receptor BRET signal (8). The suggestion that this reflected impact of that segment has not yet been confirmed with an intact Atr1a mutant. In the same previous study (8), the SecR-Atr1a hetero-receptor BRET signal was reduced by SecR TM4 and TM2 peptides and Atr1a TM4 and TM1 peptides. None of these regions have previously been confirmed in intact receptor mutant studies.

We, therefore, prepared intact SecR mutants modifying the predicted lipid face of TM2 (to complement our previous studies with similar mutations in TM4 (19)), and the intact Atr1a mutants modifying the predicted lipid faces of TM4 and TM1 to further test whether the effects of these peptides reflect the same region of their respective receptors as dominant interfaces for receptor association/oligomerization. When expressed in COS cells, all of these constructs were shown to bind their natural ligand and to signal in response to that agonist ligand similarly to the relevant wild type receptor (data not shown). As previously reported, the SecR TM4 mutant significantly reduced the SecR homo-receptor BRET signal (Fig. 3*a*) (19). However, this construct did not eliminate the Atr1a-SecR hetero-receptor BRET signal (Fig. 3*c*). The SecR TM2 mutant had no effect on either the SecR homo-receptor BRET (Fig. 3*a*) or the Atr1a-SecR hetero-receptor BRET (Fig. 3*c*) signals. Neither of the Atr1a TM segment mutants affecting only TM1 or TM4 or both TM1 and TM4 simultaneously had any effect on the Atr1a homo-receptor BRET signal (Fig. 3*b*). Of interest, both of these single TM segment mutants reduced the Atr1a-SecR hetero-receptor BRET signal, but not to background levels, whereas the construct modifying both of these TM seg-

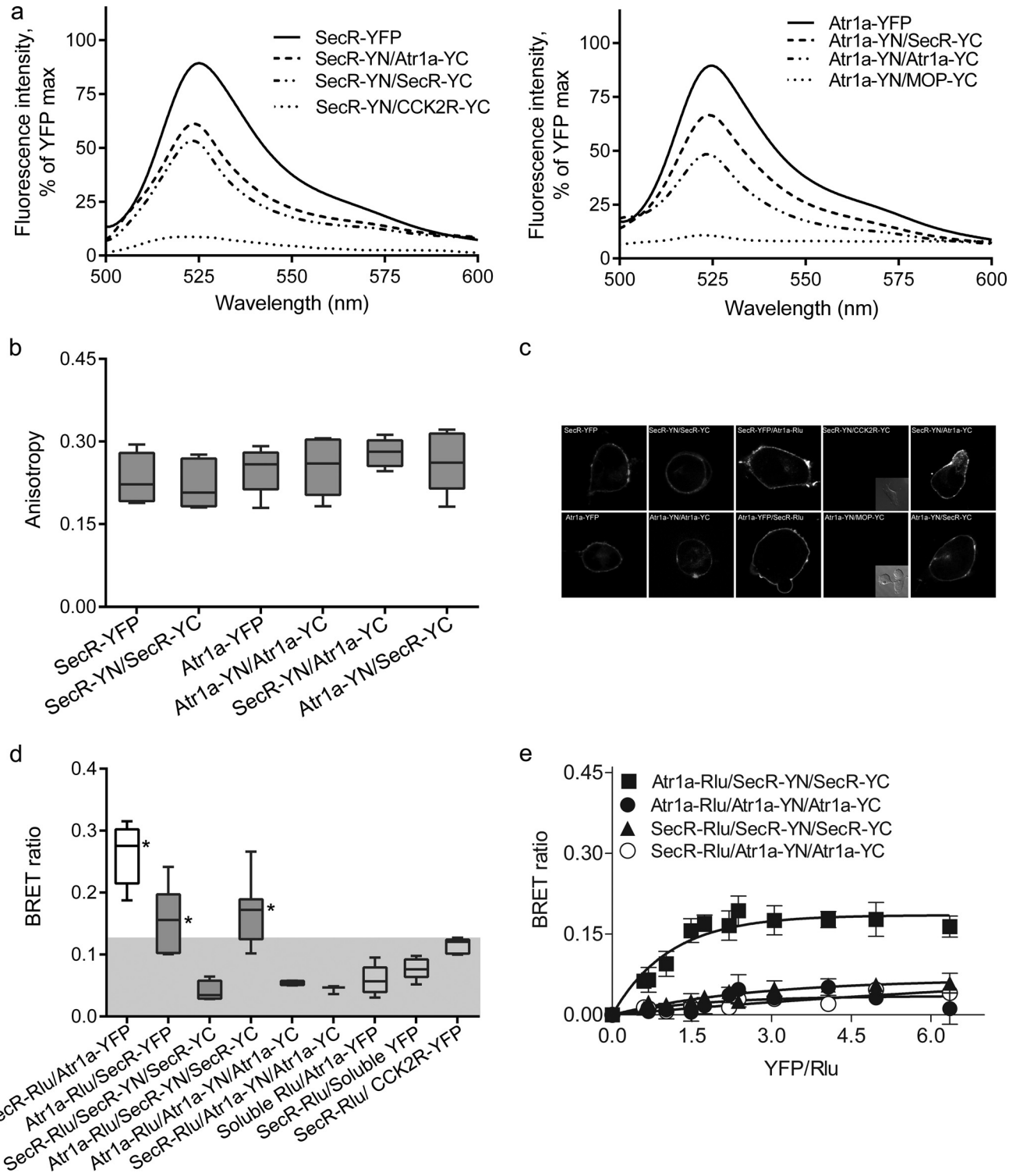

FIGURE 2. **BiFC applied to receptor complexes.** Shown are the fluorescence spectra (*panel a*), anisotropy (*panel b*), and cell surface localization of constructs (*panel c* shows fluorescence, and when not present in the control condition, an *inset* phase image of that field is included) used in these experiments. Static (*panel d*) and saturation (*panel e*) BRET signals were studied for combinations of Rlu-tagged receptor constructs co-expressed with YN- and YC-tagged receptor constructs expressed in COS-1 cells. Controls representing non-associating receptors are also shown. The cells were exposed to excitation wavelength of 480 nm and emission was measured between 500 and 600 nm. The *shaded area* represents the nonspecific BRET signal generated between soluble YFP and Rlu-tagged receptor. Data represent mean ± S.E. of 5 independent experiments performed in duplicate. * indicates BRET signals significantly above background, $p < 0.05$.

ments did fully eliminate the saturable component of this signal. Thus, it appears that at least some of the previously stated implications of the TM segment mixing experiments may have been over-interpreted (8), and the effects of those peptides may not have been through the nominal TM segments implied. Nevertheless, the Atr1a construct modifying the lipid faces of TM1 and TM4 appeared to disrupt the cross-class hetero-receptor complex between Atr1a and SecR and, as such,

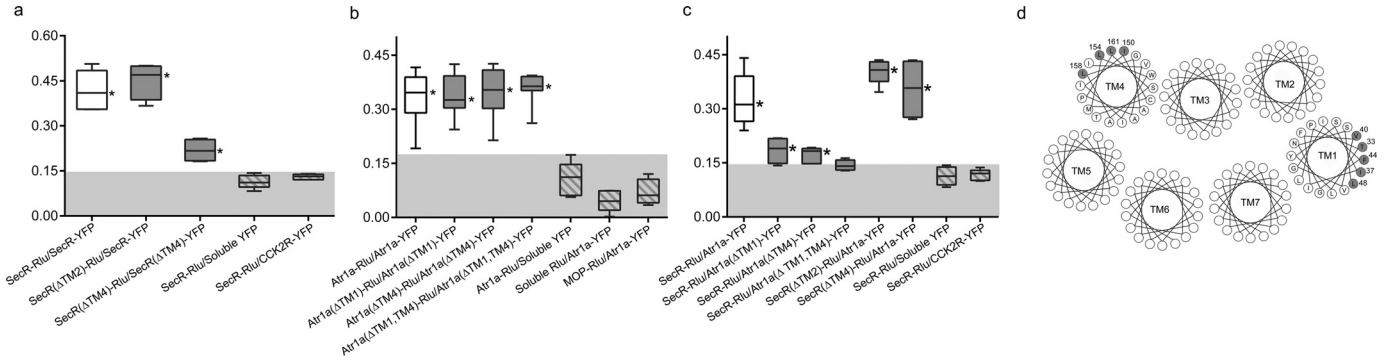

FIGURE 3. **Receptor BRET studies utilizing mutants disrupting the lipid-exposed faces of potentially important TM segments.** Shown are static BRET signals derived between Rlu- and YFP-tagged receptor constructs. *Panel a* shows possible impact on SecR-SecR homo-receptor BRET. *Panel b* shows effects on Atr1a-Atr1a homo-receptor BRET. *Panel c* shows effects on SecR-Atr1a cross-class hetero-receptor BRET. The *shaded areas* represent nonspecific BRET signals generated between tagged receptor and complementary tag in soluble form or tagged receptor and complementary tagged CCK1R known not to interact with SecR. Data represent mean ± S.E. of 4–6 independent experiments performed in duplicate. * indicates BRET signals significantly above the background, $p < 0.05$. *Panel d* shows the location of the mutations in TM1 and TM4 of Atr1a, using helical wheel display.

TABLE 1

Binding characterization of receptor-bearing CHO cell lines

SecR construct binding was characterized with ^{125}I-secretin and Atr1a construct binding was characterized with [^{125}I-Sar^1,Ile^8]ANG-II. Data are expressed as mean ± S.E. of values from 3 to 5 independent experiments. Binding sites are expressed as picomoles/mg of protein.

Cell line	Secretin affinity	Secretin B_{max}	ANG-II affinity	ANG-II B_{max}	ANG-II binding sites in cells ×10^5/cell
	pK$_i$	*pmol/mg*	*pK$_i$*	*pmol/mg*	
SecR	7.9 ± 0.1	21 ± 2	NP[a]	NP	NP/ (1.1 ± 0.2)[b]
Atr1a	NP	NP	7.8 ± 0.1	20 ± 2	1.1 ± 0.1
SecR + Atr1a (low)	8.0 ± 0.1	25 ± 2	8.5 ± 0.2[c]	3 ± 1[c]	0.4 ± 0.1
SecR + Atr1a (equal)	8.1 ± 0.2	24 ± 3	7.8 ± 0.1	22 ± 3	1.2 ± 0.1
SecR + Atr1a (high)	7.9 ± 0.1	23 ± 2	8.2 ± 0.1[c]	71 ± 11[c]	4.5 ± 0.5
SecR + Atr1a(ΔTM1, TM4) (equal)	7.7 ± 0.1	23 ± 3	7.7 ± 0.1	28 ± 2	1 ± 0.1
Atr1a(ΔTM1,TM4)	NP	NP	8.1 ± 0.2		1.2 ± 0.1

[a] NP, no saturable binding present.
[b] Secretin binding sites.
[c] $p < 0.05$ relative to Atr1a control.

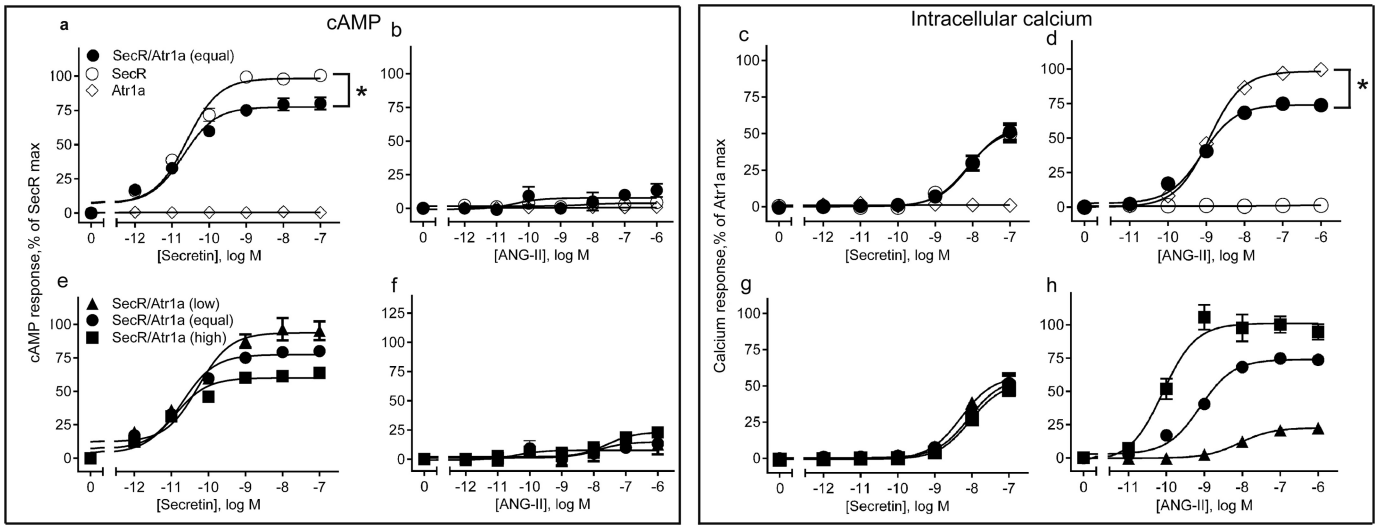

FIGURE 4. **Signaling profiles of wild type SecR and Atr1a receptor constructs.** Shown are cAMP (*left panels*) and intracellular calcium (*right panels*) signaling responses to secretin and ANG-II in receptor-bearing cell lines. Shown are data for cells expressing only a single receptor (*top row of panels*) and those expressing varied amounts of both receptors simultaneously (*bottom row of panels*). Levels of receptor expression are quantified in Table 1. Data represent mean ± S.E. of 15–28 independent experiments performed in duplicate.

should be useful to determine the physiologic functional significance of this complex. The functional characterization of the CHO cell line stably expressing approximately equal amounts of SecR and the Atr1a mutant affecting TM1 and TM4 lipid faces (Atr1a(ΔTM1,TM4)) is shown in Table 1.

To understand the functional significance of complexes involving SecR and Atr1a, it is critical to understand the signaling profiles of each receptor. We have studied secretin- and ANG-II-stimulated cAMP (Fig. 4, *a* and *b*) and intracellular calcium responses (Fig. 4, *c* and *d*) in cells expressing only one of

TABLE 2

cAMP responses to secretin in receptor-bearing CHO cell lines

Data are expressed as mean ±S.E. of values from 15 to 28 independent experiments. cAMP responses are expressed as % of SecR max.

Cell line	cAMP pEC_{50}	cAMP E_{max} [a]	cAMP pEC_{50} + ANG-II	cAMP E_{basal} + ANG-II	cAMP E_{max} + ANG-II	cAMP pEC_{50} + SII	cAMP E_{basal} + SII	cAMP E_{max} + SII
				+0.1 μM ANG-II			*+1 μM SII*	
SecR	10.6 ± 0.1	100 ± 2	NR[b]	NR	NR	NR	NR	NR
Atr1a	NR	NR	NR	NR	NR	NR	NR	NR
SecR + Atr1a (low)	10.6 ± 0.1	88 ± 4	10.5 ± 0.2	17.±5	99 ± 5	11.1 ± 0.2	14 ± 3	88 ± 9
SecR + Atr1a (equal)	10.6 ± 0.1	76 ± 4[c]	10.9 ± 0.2	10 ± 3	140 ± 6[d]	10.7 ± 0.2	11 ± 3	87 ± 7
SecR + Atr1a (high)	10.8 ± 0.1	61 ± 3[d]	10.4 ± 0.2	28 ± 6	195 ± 20[d]	10.9 ± 0.2	12 ± 5	89 ± 7[c]
SecR + Atr1a (ΔTM1,TM4) (equal)	10.4 ± 0.1	97 ± 8	10.5 ± 0.3	9 ± 2	106 ± 10	ND[e]	ND	ND
Atr1a(ΔTM1,TM4)	NR	NR	ND	ND	ND	ND	ND	ND

[a] E_{basal} , level of cAMP in absence of variable ligand; E_{max} , level of cAMP achieved in response to highest concentration of variable ligand.
[b] NR, no response.
[c] $p < 0.05$ relative to control.
[d] $p < 0.01$ relative to control.
[e] ND, not determined.

these receptors. As has been previously established (22, 23), secretin was a potent stimulant of cAMP and a weak stimulant of intracellular calcium in cells expressing SecR, but elicited no responses in cells expressing Atr1a. ANG-II was a potent stimulant of intracellular calcium in cells expressing Atr1a, whereas it elicited no intracellular calcium or cAMP responses in cells expressing SecR. Of note, the coexistence of both SecR and Atr1a in equal amounts resulted in a reduced cAMP response to secretin (Fig. 4*a*), even though the calcium response to secretin was unaffected (Fig. 4*c*). Additionally, the calcium response to ANG-II was less in the equal co-expressing line than in cells expressing only the same amount of Atr1a alone (Fig. 4*d*).

Three clonal CHO cell lines stably expressing both the SecR and Atr1a were established (binding characteristics shown in Table 1). The "equal expressor" expressed both of these receptors in densities approximating those of the lines characterized above that expressed one or the other of these receptors. The other two lines continued to express the SecR in this density, whereas varying the expression of Atr1a, with the "high Atr1a expressor" expressing a stoichiometric excess of that receptor over SecR and the "low Atr1a expressor" expressing a stoichiometric excess of SecR over Atr1a. We also prepared a cell line expressing SecR and the Atr1a mutant changing the lipid-facing surfaces of TM1 and TM4 discussed above, with both of these receptors in similar densities to each other and to match those in the single and equal expressing cell lines.

The functional characterization of these co-expressing cell lines is also shown in Fig. 4 (cAMP responses in Fig. 4, *e* and *f*, intracellular calcium responses in Fig. 4, *g* and *h*), with quantitation of relevant parameters listed in Tables 2 and 3. Co-expression of the SecR with increasing amounts of Atr1a resulted in progressive reduction in secretin-stimulated cAMP responses as the density of Atr1a increased (Fig. 4*e*). In contrast, the presence of Atr1a had no impact on secretin-stimulated intracellular calcium responses in these cell lines (Fig. 4*g*). This suggested that Atr1a was acting as a negative allosteric modulator of secretin-stimulated cAMP at SecR, with a functionally biased effect, because intracellular calcium responses to this agonist was not affected. The ANG-II-stimulated intracellular calcium responses correlated with the density of Atr1a (Fig. 4*h*). However, because expression of the same density of Atr1a in the presence of SecR than in its absence resulted in a lower calcium response to ANG-II (Fig. 4*d*), it appears that the Atr1a-SecR hetero-receptor complexes either reduced or eliminated the calcium response to ANG-II.

The same three stoichiometrically defined cell lines were also studied in the presence of agonist occupation (saturating concentration) of one of the two co-expressed receptors (Fig. 5). The *left six panels* reflect cAMP responses (Fig. 5, *a–f*) and the *right six panels* (Fig. 5, *g–l*) reflect intracellular calcium responses, with the left column in each set showing an effect of ANG-II occupation on secretin responses and the right column showing effect of secretin occupation on ANG-II responses. Secretin-stimulated cAMP responses were increased by occupation of Atr1a with ANG-II (Fig. 5, *a*, *c*, and *e*). This effect was not significant for the low Atr1a expressor line, but had progressively more impact as the level of Atr1a increased. In contrast, whereas ANG-II increased the basal levels of intracellular calcium in these lines, correlating with the density of Atr1a present (Fig. 5, *g*, *i*, and *k*), the impact of secretin stimulation was only positive for the low Atr1a expressor line (Fig. 5*g*) and secretin had no effect or tended to reduce the intracellular calcium response for those lines expressing more Atr1a (Fig. 5, *i* and *k*).

Consistent with the negative impact of Atr1a on secretin-stimulated cAMP responses, the same concentration of secretin (0.1 μM) resulted in progressively lower basal levels of cAMP in the absence of ANG-II (Fig. 5, *b*, *d*, and *f*), whereas increasing stimulation with ANG-II then stimulated the cAMP responses to maximal in all three cell lines. Note that ANG-II normally does not increase cAMP levels at either of these receptors. The intracellular calcium responses in the presence of secretin occupation of SecR were only additive of those occurring at the component-isolated receptors (Fig. 5, *h*, *j*, and *l*).

The possible impact of SII was also explored (Fig. 6). Secretin-stimulated cAMP responses (Fig. 6, *a-c*) were not significantly affected by agonist occupation of Atr1a with this ligand, SII, until there was a stoichiometric excess of the latter receptor present. In the high Atr1a expressor line, the SII-occupied Atr1a increased the secretin-stimulated cAMP response (Fig. 6*c*), essentially reversing the negative impact of co-expression of these receptors. In contrast, secretin-stimulated intracellular calcium responses were not significantly different in the presence of SII (Fig. 6, *d–f*). Under these assay conditions, SII did not stimulate an intracellular calcium response in any of these cell lines (Fig. 6, *g–i*).

TABLE 3

Intracellular calcium responses to secretin and ANG-II in receptor-bearing CHO cell lines

Data are expressed as mean ±S.E. of values from 15 to 25 independent experiments. Intracellular calcium responses are expressed as % of Atr1a max.

Cell line	Secretin stimulation							ANG-II stimulation				
	Calcium pEC_{50}	Calcium E_{max} [a]	Calcium pEC_{50} +ANG-II	Calcium E_{basal} + ANG-II	Calcium E_{max} + ANG-II	Calcium pEC_{50} + SII	Calcium E_{max} +SII	Calcium pEC_{50}	Calcium E_{max}	Calcium pEC_{50} + Sec	Calcium E_{basal} + Sec	Calcium E_{max} + Sec
				+0.1 μM ANG-II			*+1 μM SII*				*+0.1 μM Sec*	
SecR	8.3 ± 0.1	50 ± 6	ND[b]	ND	ND	ND	ND	NR[c]	NR	ND	ND	ND
Atr1a	NR	NR	ND	ND	ND	ND	ND	8.9 ± 0.1	100 ± 2	ND	ND	ND
SecR + Atr1a (low)	8.3 ± 0.1	55 ± 5	9.0 ± 0.3	29 ± 4	73 ± 11	8.2 ± 0.1	36 ± 6	7.9 ± 0.1	25 ± 3[d]	ND	35 ± 4	48 ± 5
SecR + Atr1a (equal)	8.2 ± 0.1	53 ± 6	ND	60 ± 4	50 ± 1	8.3 ± 0.1	28 ± 2	9.2 ± 0.1	77 ± 2[d]	8.9 ± 0.1	25 ± 5	76 ± 8
SecR + Atr1a (high)	8.1 ± 0.1	45 ± 5	ND	86 ± 5	68 ± 9	8.3 ± 0.1	68 ± 9	9.9 ± 0.1[d]	102 ± 7	10.2 ± 0.3	26 ± 6	87 ± 9
SecR + Atr1a (ΔTM1,TM4) (equal)	8.1 ± 0.1	38 ± 4	ND	ND	ND	ND	ND	8.6 ± 0.1	91 ± 4	ND	ND	ND
Atr1a (ΔTM1, TM4)	NR	NR	ND	ND	ND	ND	ND	8.1 ± 0.1	92 ± 2	ND	ND	ND

[a] E_{basal}, level of calcium in absence of variable ligand; E_{max}, level of calcium achieved in response to highest concentration of variable ligand.
[b] ND, not determined.
[c] NR, no response.
[d] $p < 0.05$ relative to control.

The Atr1a mutant in which the lipid-facing residues of TM1 and TM4 were modified to disrupt interactions between Atr1a and SecR provided a highly useful tool to further explore the functional impact of the hetero-receptor complex. Because it bound ANG-II and signaled like wild type Atr1a, it also provided the opportunity to explore whether modulatory effects were likely generated at the level of the receptor interaction or could have been more distal along the signaling pathways. Full concentration-responses curves for stimulating cAMP (Fig. 7, *a*, *b*, *e*, and *f*) and intracellular calcium (Fig. 7, *c*, *d*, *g*, and *h*) are illustrated in Fig. 7 with quantitation of relevant parameters in Tables 2 and 3. The top row (Fig. 7, *a–d*) shows the responses for this Atr1a mutant when expressed alone. Under these conditions, this mutant exhibited no cAMP responses to either secretin or ANG-II (Fig. 7, *a* and *b*). Secretin did not elicit intracellular calcium responses at this mutant (Fig. 7*c*), whereas ANG-II stimulated identical intracellular calcium responses at this mutant and at wild type Atr1a (Fig. 7*d*). Note also that the intracellular calcium responses were substantially to the right of the cAMP responses in these concentration-response curves. At the agonist concentrations that stimulate maximal cAMP responses, minimal or no intracellular calcium responses were observed. The bottom row of panels illustrates the effects of co-expression of these receptors. The negative impact of co-expression of SecR and Atr1a on secretin-stimulated cAMP responses was reversed by disrupting this complex with the Atr1a mutant (Fig. 7*e*). Furthermore, the positive impact of ANG-II on secretin-stimulated cAMP responses was also reversed by disrupting this complex (Fig. 7*f*). The negative impact of SecR expression on the intracellular calcium response to ANG-II at the Atr1a was also eliminated when the mutant Atr1a was introduced (Fig. 7*h*).

Discussion

A functionally important cross-class G protein-coupled hetero-receptor complex including the class A Atr1a and class B SecR was recently reported (8), yet the characterization of this complex was quite limited (8). Additionally, possible interfaces between the interacting receptors were implied based on mixing with transmembrane (TM) segment peptides and assuming that these competed for the nominal portion of the relevant receptors, but this was not previously definitively established. In the current work, we have advanced our understanding of the structure and function of the complexes involving Atr1a and SecR, using a variety of fluorescence and biochemical techniques and a series of well characterized cell lines expressing different stoichiometric ratios of these two receptors. We now establish that at least some of the inferences based on the competitive use of TM peptides were not correct, and that there are a variety of complexes that likely exist in a dynamic equilibrium. The dominant complex is now shown to involve a stable core of the SecR homodimer decorated by monomeric Atr1a through the external lipid-directed faces of TM1 and TM4 of Atr1a, with disruption of each individually not able to fully eliminate these complexes.

The physiologic relevance of SecR-Atr1a hetero-receptor complexes has previously been established, based on *in vivo* experiments with peptide and receptor knock-out animals (9,

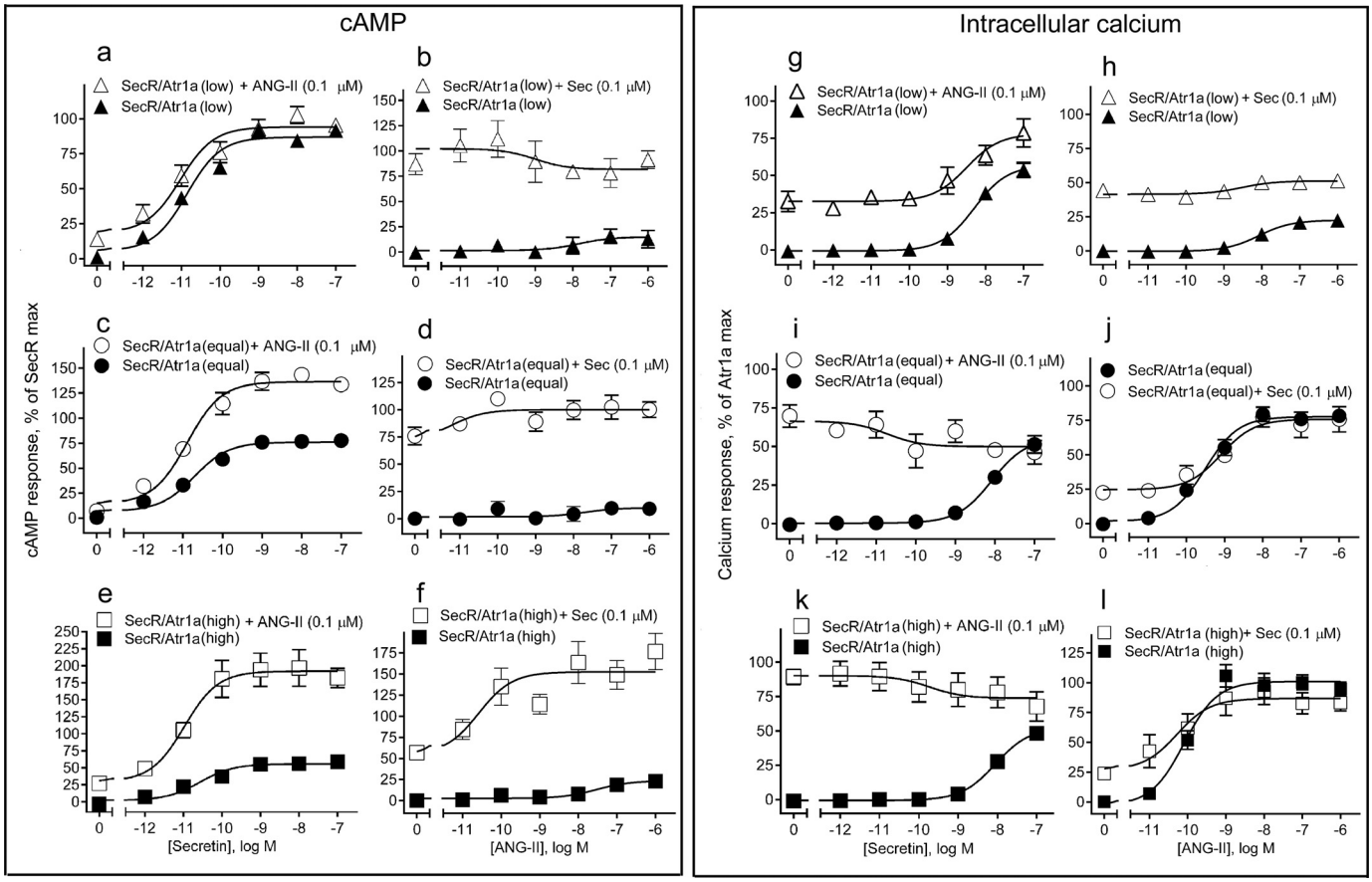

FIGURE 5. **Impact of angiotensin and secretin on agonist-stimulated signaling profiles of SecR-Atr1a co-expressing cells.** Shown in the *left panels* are cAMP responses to a variety of secretin concentrations in the presence of 0.1 μM ANG-II and a variety of ANG-II concentrations in the presence of 0.1 μM secretin in the cell lines co-expressing SecR and low, equal, or high levels of Atr1a. Shown in the *right panels* are intracellular calcium responses under the same conditions in the same cell lines. Data represent mean ± S.E. of 15–25 independent experiments performed in duplicate.

12), and intra-cerebroventricular injections of hormones (24). ANG-II and secretin have been shown to share overlapping and interdependent osmoregulatory roles in the brain, where both secretin and its receptor are required for the classical effect of ANG-II to stimulate drinking behavior when the organism is exposed to hyperosmolality (25). Various manipulations, such as disruption of complexes involving both receptors without removing the receptors from the cell surface (19), have suggested that the interdependence originates at this cross-class receptor complex, rather than through interactions of post-receptor signaling pathways. This emphasizes the importance of further characterization of the complex, as well as strategies to disrupt it that might ultimately be testable in physiologic systems.

Peptides representing transmembrane segments of receptors have been utilized to compete for protein-protein interactions involving that segment (26). This can be validated using mutants of the relevant face of the peptide, thereby eliminating the effect, and by modifying the relevant region within an intact receptor, also eliminating the effect. In the earlier report first describing direct interactions between Atr1a and SecR (8), the first two steps were followed, but not the third. In the current work, we have prepared and studied intact receptors with mutations in the lipid-facing region of the TM segments of interest. Unexpectedly, the Atr1a TM4 mutant, representing the TM segment peptide that disrupted Atr1a-Atr1a BRET (8), did not have any effect on homodimerization of Atr1a evaluated by intact receptor BRET. Both the Atr1a TM1 and TM4 segment mutants partially inhibited the Atr1a-SecR BRET, with the combination of the two mutants completely eliminating the specific BRET signal. In the previous peptide competition studies (8), each of these peptides was able to eliminate this signal by itself. Similarly, the SecR TM2 mutant had no effect on Atr1a-SecR BRET, whereas it had reduced the same BRET signal when the peptide had been utilized previously (8). Although lack of confirmation of some of these previous interpretations is disappointing, at least the clues provided by those studies were useful in the current work for the successful preparation of an Atr1a mutant that was able to eliminate any BRET evidence of Atr1a-SecR stable association, whereas not having any negative impact on ANG-II binding or biological activity at that receptor. This has provided a much needed tool for further studies of the functional impact of this hetero-receptor complex.

Studying the functional impact of a hetero-receptor complex is quite challenging, because the co-expression of both receptors involved in the complex on the same cell results in a variety of states of association. As shown in Fig. 8, both Atr1a and SecR can exist both as monomers and as homodimers (and perhaps higher order oligomers for Atr1a). Hetero-receptor complexes can take the form of associated monomers, monomers associ-

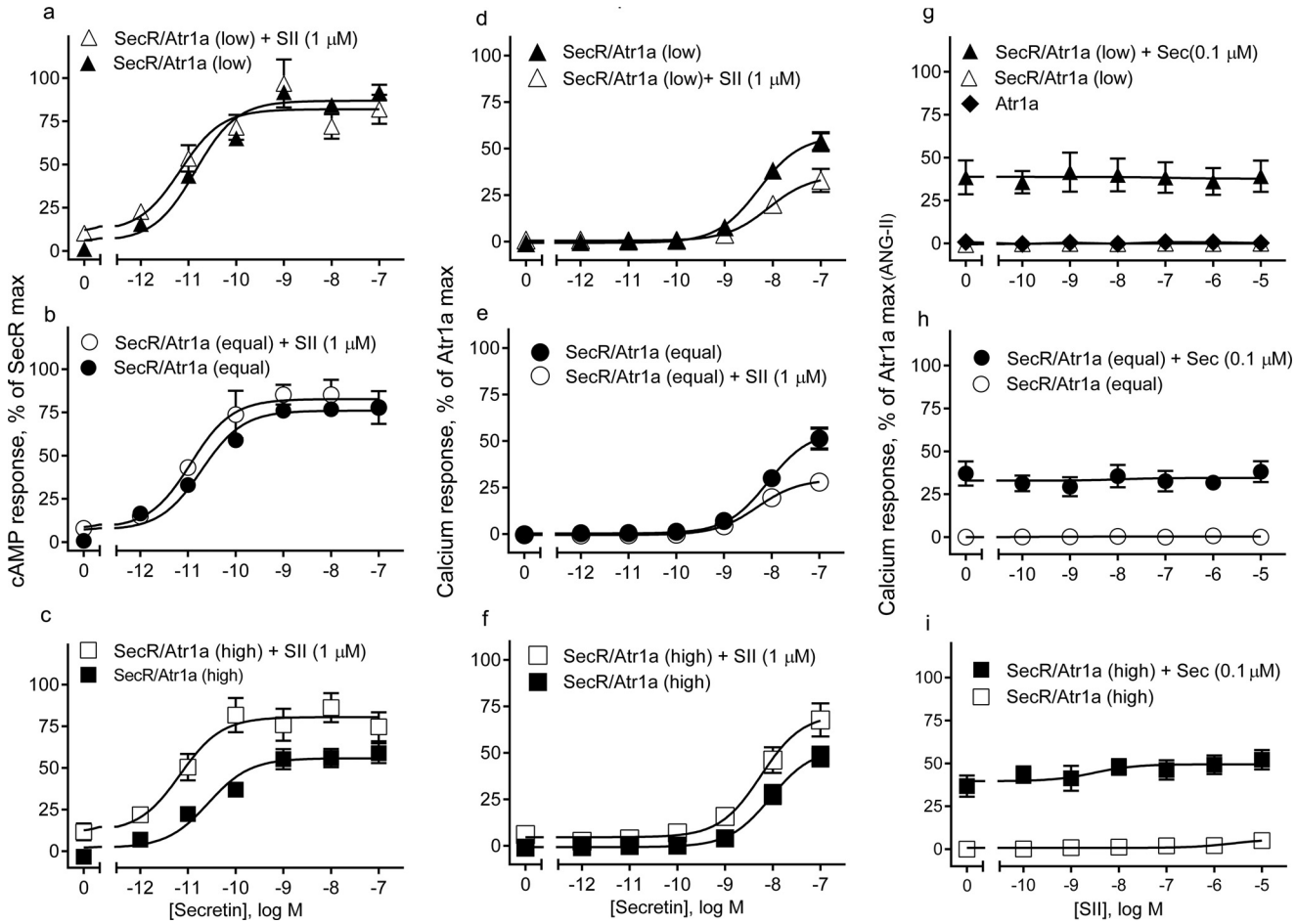

FIGURE 6. **Impact of SII on secretin-stimulated signaling profiles of SecR-Atr1a co-expressing cells.** Shown are cAMP and intracellular calcium responses to a variety of secretin concentrations (*panels a–f*) in the presence of the β-arrestin-biased agonist, SII (1 μM), in cell lines co-expressing SecR and low, equal, or high levels of Atr1a. Also shown in *panels g–i* are the absent intracellular calcium responses in these cells to SII. Data represent mean ± S.E. of 10–15 independent experiments performed in duplicate.

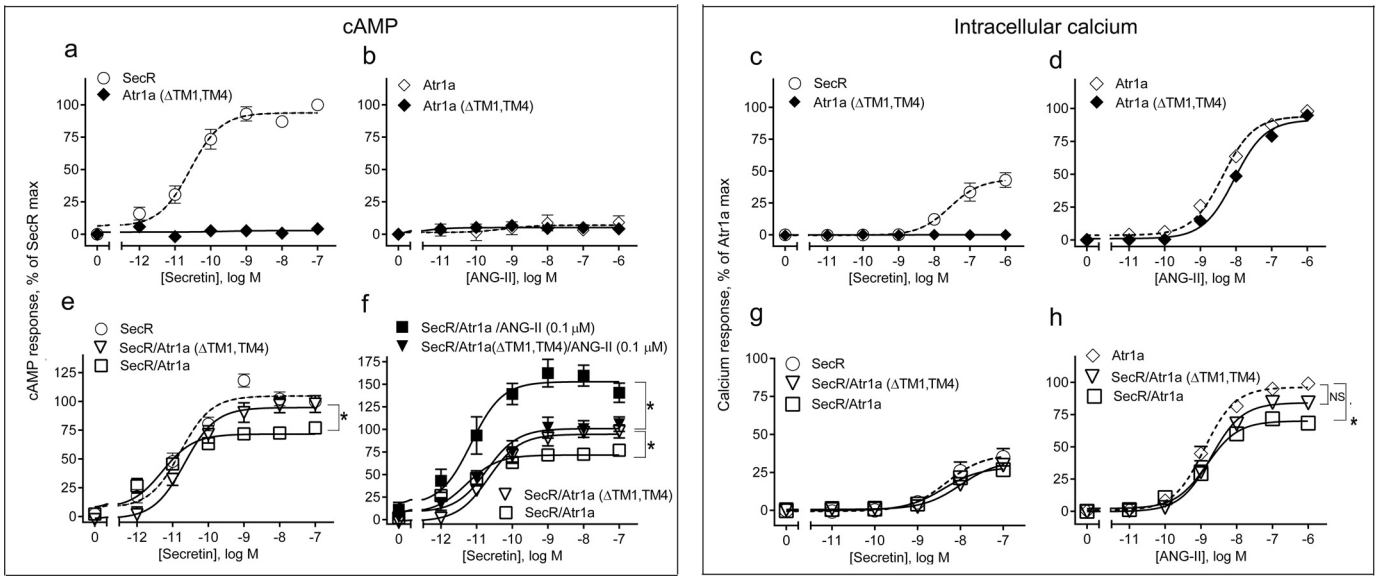

FIGURE 7. **Signaling studies using the non-associating Atr1a mutant.** Shown are cAMP and intracellular calcium responses to secretin and ANG-II in cell lines expressing the Atr1a mutant affecting TM1 and TM4 alone or as co-expressed with SecR. Stable cell lines expressing similar numbers of both receptors are studied (characteristics shown in Table 1). The *top row* illustrates the signaling characteristics of this mutant Atr1a when expressed alone, whereas the *bottom row* illustrates the signaling characteristics of co-expression of receptors, as noted. Data represent mean ± S.E. of 6–15 independent experiments performed in duplicate. * indicates maximal cAMP or intracellular calcium responses that are significantly different from the noted control, $p < 0.05$.

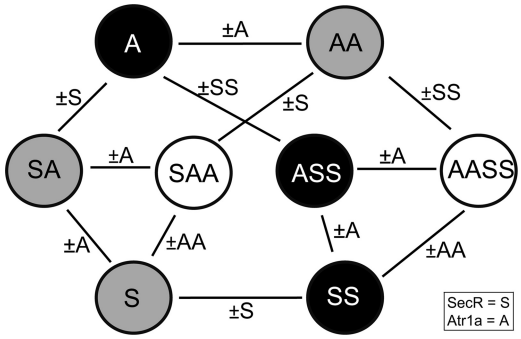

FIGURE 8. **Possible monomeric and oligomeric states of Atr1a and SecR.** Shown are the various states of these receptors when expressed on the same cell. Both GPCRs are known to exist as monomeric forms and to be capable of interacting with themselves and with each other. SecR is known to exist predominantly in a homodimeric state, and not to form higher order oligomers (20). Atr1a can transiently associate with itself and, like many class A GPCRs, may go on to form higher order complexes (these are not represented in the diagram for purposes of simplicity and because no such complexes have been definitively identified). Major states are shown as *black circles with white lettering*, whereas other states likely to exist at some intermediate level of importance are shown with *gray shading*.

ating with dimers, and dimers associating with dimers, and perhaps even more complex forms. Within any of these complexes, there is also the possibility of having various distinct interfaces between the interacting partners. A clear example of this is that Atr1a can interact with SecR through its TM1 and TM4 interfaces. We do not know whether such complexes may even have functions that are distinct from each other.

The best current insights suggest that the predominant cross-class receptor complex represents Atr1a decorating an intact symmetrical SecR-SecR homodimer that is formed along its TM4 interface. Although the core of such a complex is relatively stable and structurally well defined, the interface with the modulating Atr1a is less stable and less well defined. There is good evidence that both the lipid-exposed faces of TM1 and TM4 of Atr1a contribute to this complex and that disruption of both must occur before the complex is largely eliminated. The latter mutant Atr1a is a very important tool that can potentially be utilized to explore the *in vivo* impact of this complex without interfering with the independent functions of either component receptor.

This cross-class complex of GPCRs is shown to be associated with a reduced ability of secretin to stimulate a cAMP response, unless the Atr1a is in its activated state, in which case the same responses were observed to be amplified. Atr1a activated by agonist occupation (or a constitutively active mutant (8)) resulted in enhanced cAMP responses to secretin. This enhanced cAMP response could reflect either direct allosteric modulation at the level of receptor-receptor interaction or impact of downstream signaling events. Indeed, whereas ANG-II does not directly couple with G_s and stimulate adenylate cyclase to yield an increase in cAMP, it does couple with G_q and result in increased intracellular calcium as well as activation of protein kinase C. Protein kinase C can sensitize adenylate cyclase, and this can theoretically augment the cAMP response to ANG-II (27).

For this reason, it was important to identify a variant of Atr1a that bound ANG-II and signaled like wild type receptor, yet that was less likely (or unable) to form the cross-class receptor complexes with SecR. Indeed, Atr1a (ΔTM1,TM4) was shown to have these properties. Of note, when it was co-expressed with equal numbers of SecR on the CHO cell line, analogous to the co-expressing wild type receptor-bearing line, there were marked functional differences. All of the modulatory events described above were absent in the mutant receptor-bearing line, whereas they were present in the wild type receptor-bearing line. This provides strong evidence for these effects being dependent on receptor-receptor interaction and reflecting lateral allosteric modulation events.

It is possible that the absence of measurable intracellular calcium events reflects the sensitivity of the assay, rather than true absence of activation of that pathway. Indeed, development of very sensitive techniques to examine receptor-G protein interaction (27) has shown that SII is actually a partial agonist of G protein activation at Atr1a, with evidence of ability to couple with G_q and G_i. Yet, under the conditions of study in this work, no significant calcium response was observed for SII. Similarly, the concentration-response curves for stimulating intracellular calcium by ANG-II were far to the right of the curves for stimulation of cAMP. This suggests the presence of little or no activation of the G_q pathway under conditions in which G_s was activated, and provides some further support for the impact on cAMP responses to not be mediated by PKC.

Thus, the Atr1a plays dual allosteric modulatory roles, both as a negative allosteric modulator when it is in an inactive state and as a positive allosteric modulator when it is in an activated state. Furthermore, this modulator possesses bias in its effects, modulating cAMP responses, whereas having quite distinct impact on intracellular calcium responses. Current data suggests that involvement in such a complex reduces or eliminates the ability of ANG-II to stimulate an intracellular response at the Atr1a.

Of particular interest, in the hetero-receptor complex, ANG-II was able to elicit a cAMP response, something it was unable to do when stimulating cells expressing only Atr1a or only SecR. This might be a key observation to explain how ANG-II stimulated drinking behavior in a normal animal that expresses both of these receptors in the key osmoregulatory centers. It also provides an explanation for the requirement of SecR for the drinking effect of ANG-II observed in knock-out animals (9). Perhaps the additional requirement for secretin peptide that was observed in secretin peptide knock-out animals (12) relates to its provision of a basal tone of activation that might also be necessary.

Experimental Procedures

Materials—Molecular biology reagents were from New England BioLabs (Ipswich, MA). Coelenterazine *h* was from QT (Hayward, CA). cAMP assay kits using Lance Technology and Optiplates were from PerkinElmer Life Sciences (Wellesley, MA). Quest Fluo-8-AM™ was from AAT Bioquest Inc. (Sunnyvale, CA). Polyethyleneimine was from Polysciences, Inc. (Warrington, PA). Clear-bottom black 96-well tissue culture plates were from Corning. Lipofectamine™ LTX and Plus™ reagent, Ham's F-12 medium, Dulbecco's modified Eagle's medium (DMEM), minimum essential medium, and zeocin were from Invitrogen (Carlsbad, CA) and fetal clone II

supplement was from Hyclone Laboratories, (Logan, UT). Other reagents were analytical grade.

Peptides—Rat secretin(1–27) and [Tyr^{10}]secretin (for radioiodination) were synthesized in our laboratory. ANG-II and [Sar^{1},Ile^{8}]angiotensin-II (for radioiodination) were purchased from Phoenix Pharmaceuticals Inc. (Burlingame, CA), and [Sar^{1},Ile^{4},Ile^{8}]angiotensin-II (SII) (a β-arrestin-biased agonist and partial agonist of G protein activation of the angiotensin receptor (27)) was from Bachem (Torrance, CA).

Receptor Constructs—Mouse SecR and mouse Atr1a constructs, and those tagged at their carboxyl terminus with *Renilla* luciferase (Rlu), yellow fluorescent protein (YFP), N-terminal half of yellow fluorescent protein (YN), or C-terminal half of yellow fluorescent protein (YC) were subcloned into pcDNA3.0 eukaryotic expression vectors. All sequences were confirmed by DNA sequencing. Constructs representing the human type 1 cholecystokinin receptor (CCK1R) or human type 2 cholecystokinin receptor (CCK2R) tagged at the carboxyl terminus with Rlu and YFP (16) and the μ-opioid receptor tagged at the carboxyl terminus with Rlu were also utilized as non-associating receptor controls.

Alanine-replacement mutagenesis of various lipid-facing residues of Atr1a was performed using QuikChange site-directed mutagenesis (Agilent Technologies, Santa Clara, CA), with sites identified based on a homology model of the crystal structure of CXCR1. These included alanine replacements for the Atr1a TM1 segment residues Thr^{33}, Ile^{37}, Val^{40}, Phe^{44}, Leu^{48}, and TM4 segment residues Ile^{150}, Leu^{154}, Leu^{158}, and Leu^{161} (see helical wheel diagram in Fig. 3*d*). A similar approach was taken for the mutagenesis of SecR TM2 residues Val^{197}, Leu^{201}, Leu^{204}, Ile^{208}, as well as for TM4 segment residues Gly^{256} and Ile^{260}, following the work previously described (19).

Cell Culture and Transfections—African green monkey kidney (COS-1) cells or human embryonic kidney (HEK293) cells were used for transient expression of receptor constructs. Cells were grown in sterile 10-cm tissue culture plates in DMEM supplemented with 5% fetal clone II (COS-1 cells) or minimum essential medium supplemented with 10% fetal bovine serum (HEK293 cells) in a 37 °C incubator in a humidified environment containing 5% carbon dioxide. When the cells reached approximate confluence of 80%, they were transfected with 1.5 μg of DNA per plate using the established DEAE-dextran method (28).

Stable Co-expression of SecR-Atr1a Receptor—Chinese hamster ovary (CHO) cell lines were engineered to stably express either mouse SecR or Atr1a or both Atr1a and SecR constructs, using the approach we described previously (28). The parental CHO cells not expressing either of these receptors were transfected using Lipofectamine LTX and Plus reagent in Opti-MEM following the manufacturer's instructions. Stably expressing receptor clones were chosen after initial selection using either G-418 or zeocin (1 mg/ml). For dual receptor expression, cell lines expressing SecR were subsequently transfected with Atr1a construct and clones were enriched using zeocin, followed by cloning using limiting dilution. We chose SecR-expressing and Atr1a-expressing cell lines having similar numbers of receptors based on radioligand binding assays. In the case of dual receptor-expressing cell lines, we have carefully selected a series of SecR-Atr1a cell lines based on low, equal, or high Atr1a receptor number (relative to those of SecR) in the background of clonal CHO-SecR cells. Receptor expression levels in these cell lines were characterized using radioligand binding assays (described below).

These cell lines were grown at 37 °C in tissue culture flasks containing Ham's F-12 medium supplemented with 5% fetal clone II in a humidified environment containing 5% carbon dioxide. Cells were passaged approximately two times per week.

Fluorescence Microscopy—Levels of receptor expression in specific cellular compartments and the combination of YN and YC to yield an intact fluorophore were evaluated by monitoring YFP fluorescence. Receptor-bearing HEK293 cells grown on a 25-mm coverslips were washed with phosphate-buffered saline (PBS) and were fixed in 2% (w/v) paraformaldehyde in PBS for 20 min. Coverslips were mounted on microscopic slides using vectashield (Vector Laboratories, Burlingame, CA). Cell surface fluorescence images were acquired using a Zeiss LSM510 (Thornwood, NY) confocal microscope (pinhole diameter of 220 μm with a plan-apochromat $\times$63 1.3 numerical aperture oil objective) configured to capture YFP (excitation 488 nm, emission 500–550 nm band pass filter). In the absence of substantial fluorescence, phase images of the relevant field were acquired. The final images were assembled and organized using Adobe Photoshop version 7.0.

Fluorescence Spectroscopy and Anisotropy—Steady-state fluorescence spectra of fluorescent receptor-bearing COS cells were recorded using a Fluoromax-3 fluorometer (SPEX industries, Edison, NJ) at 25 °C with a 1-ml quartz cuvette. The medium used for cell suspension was degassed by bubbling nitrogen. Experimental data were corrected by subtracting data from analogous experiments performed with untransfected COS cells to reflect the effects of light scattering and background.

Steady-state anisotropy measurements were recorded with the same fluorometer equipped with polarizers. Measurements were performed with excitation wavelength of 480 nm (6.8-nm bandwidth) and emission wavelength of 525 nm. Emission intensities were measured with excitation-side polarizer in the vertical position and emission-side polarizer in horizontal and vertical positions.

Receptor BRET Studies—BRET studies were performed in transfected COS-1 cells, due to the large number of different experimental and control conditions needed for study. Cells expressing both donor and acceptor constructs were used for bioluminescence and fluorescence measurements in 96-well white Optiplates, as described previously (19). The cells were studied 48 h after transfection. The static BRET assays were initiated by mixing the cells with 5 μM coelenterazine *h (Renilla* luciferase-specific substrate) at room temperature. The emission signals were acquired using a 2103 Envision fluorescence plate reader configured with the <700 nm mirror and with dual emission filter sets for luminescence (460 nm, bandwidth 25 nm) and fluorescence (535 nm, bandwidth 25 nm). The absolute BRET ratios were calculated based on ratios of YFP and Rlu emission signals, as described previously (19). Background BRET for the experimental system was determined using solu-

ble complementary donor or acceptor, as well as paired structurally unrelated receptors previously demonstrated to not associate with the experimental receptor of interest (CCK2R with SecR and μ-opioid receptor with Atr1a). An additional control represented BRET with both donor and acceptor for a structurally unrelated class A GPCR, CCK1R, also known not to interact with SecR (16), and examining the ability of SecR to affect this signal.

Saturation BRET experiments were also performed as described previously (19). Here, the COS-1 cells were transfected with a fixed amount of Rlu-tagged receptor constructs as fluorescence donors (0.75 μg DNA/plate) and with increasing amounts of YFP-tagged constructs as fluorescence acceptors (0.15 to 3 μg of DNA/plate) or with a combination of YN- and YC-tagged constructs. The BRET signals were collected as described above, and the BRET ratios were calculated and plotted against the ratios of Rlu/YFP, with the curves fitted and evaluated based on R^2 values using Prism 6.0 (GraphPad, San Diego, CA).

Competition experiments using unlabeled receptor constructs also provided insights into the stability of the oligomeric receptor complex and the ease of disrupting it. These experiments were performed after the cells were transfected with 1 μg each of Rlu-tagged donor construct and YFP-tagged acceptor construct, along with various amounts of competitive untagged receptors, as noted (ranging from 0.5 to 8 μg). Levels of YFP fluorescence indicated that levels of SecR and Atr1a receptor expression were similar under all conditions studied. These data were expressed as percentages of the specific receptor BRET signal in the absence of competitor, subtracting the background BRET signal determined as described above.

Receptor-enriched Cell Membranes—Membrane fractions were isolated from the receptor-bearing CHO cells as described previously (28). Cells at approximate 80–90% confluence were harvested mechanically using a cell scraper and were suspended in ice-cold PBS, pH 7.4. The fraction of interest was isolated using discontinuous sucrose density gradient centrifugation, and membranes were suspended in Krebs-Ringer-HEPES (KRH) medium (25 mM HEPES, pH 7.4, 104 mM NaCl, 5 mM KCl, 1.5 mM $CaCl_2$, 1.0 mM KH_2PO_4, 1.2 mM $MgSO_4$, 1.2 mM $MgCl_2$) containing 0.01% soybean trypsin inhibitor and 1 mM phenylmethylsulfonyl fluoride. Membranes were stored at −80 °C until use.

Receptor-binding Assays—Receptor binding studies were performed using cell membranes or intact cells, as described previously (19). Membranes were mixed with ~5 pM [^{125}I-Sar^1,Ile^8]angiotensin-II or [^{125}I-Tyr^{10}]secretin (prepared and purified in our laboratory to yield approximate specific radioactivity of 2,000 Ci/mmol) in the absence or presence of increasing concentrations (0 to 1 μM) of unlabeled ligands for 1 h at room temperature in KRH medium, pH 7.4, containing 0.01% soybean trypsin inhibitor and 0.2% bovine serum albumin. The receptor-bound fraction was separated from free radioligand using centrifugation and repeated washing with ice-cold KRH medium. Receptor-bound radioactivity was quantified using a γ-spectrometer. Non-saturable binding was determined in the presence of 1 μM unlabeled ligand, and represented less than 15% total binding. Saturable binding data were analyzed using the LIGAND program and were plotted using the non-linear least-squares curve-fitting routine in Prism 6.0 (GraphPad, San Diego, CA). Intact cell binding was performed and analyzed similarly, to determine receptor density on the cell surface.

Intracellular Calcium Assays—Agonist-stimulated biological activity was quantified by measuring the intracellular calcium responses in intact cells. Receptor-bearing CHO cells were seeded in sterile clear-bottom black 96-well tissue culture plates 24 h before the assay. When ~80% confluent, cells were washed with KRH medium containing 2.5 mM probenecid and 0.2% bovine serum albumin, and were incubated with 0.75 μM Quest Fluo 8 (dissolved in anhydrous dimethyl sulfoxide) at 37 °C for 1 h in the dark. Incubations were terminated by aspirating the medium and washing the cells with KRH medium containing 0.2% bovine serum albumin. The calcium response assay was initiated by addition of agonist. Assays were performed in a FlexStation 3.0 plate reader (Molecular Devices, Sunnyvale, CA) using robotic addition of the appropriate agonist ligand (secretin or ANG-II). Calcium responses were measured at 37 °C by quantifying the fluorescence emission intensity at 525 nm after exciting the samples at 485 nm, with data collection every 4 s over a 120-s period. The impact of ANG-II (or SII) on the secretin-stimulated calcium responses were measured by simultaneous addition of both secretin (0 to 100 nM) and ANG-II (0.1 μM) (or 1 μM SII). Similarly, the impact of secretin (0.1 μM) on the ANG-II (0 to 1 μM)-stimulated calcium responses were carried out by simultaneous addition of both ligands. Data were plotted using Prism 6, and concentration-dependent responses were evaluated.

cAMP Assays—Agonist-stimulated cAMP accumulation in receptor-bearing CHO cells was quantified using the LANCE assay from PerkinElmer, with assays performed in 384-well white Optiplates using a 2103 Envision plate reader (PerkinElmer), as described previously (20). Receptor-bearing cells were plated 24 h before stimulation on sterile 96-well clear plates and assayed when ~80% confluent. Cells were stimulated with increasing concentrations of secretin (0 to 100 nM) or ANG-II (0 to 1 μM) in KRH medium, pH 7.4, containing 0.2% bovine serum albumin, 0.01% soybean trypsin inhibitor, 0.1% bacitracin, and 1 mM 3-isobutyl-1-methylxanthine for 30 min at 37 °C. After 30 min, the incubations were terminated by addition of 6% ice-cold perchloric acid, and the pH was adjusted to 6.5 using 30% $KHCO_3$. The cAMP assay was performed using 6 μl of cell supernatant mixed with an equal volume of Alexa Fluor® 647-labeled cAMP antibodies in KRH medium containing 0.05% bovine serum albumin and incubated for 30 min at room temperature in the dark. This was subsequently mixed with 12 μl of detection solution containing biotin-cAMP and europium-labeled streptavidin. Time-resolved FRET signals were measured in a 2103 Envision plate reader (PerkinElmer) after excitation at 340 nm, with emission measured at 615 and 665 nm wavelengths.

Statistical Analysis—Unless specifically noted, differences between two experimental conditions were evaluated using unpaired *t* tests or analysis of variance with Dunn's multiple comparison tests in Prism 6. A value of $p < 0.05$ was considered to be statistically significant.

Author Contributions—K. G. H. and L. J. M. designed the study. K. G. H. and M. L. A. performed the experiments and data analysis. K. G. H., L. T. O. L., B. K. C. C., and L. J. M. wrote the manuscript. All authors approved the final version of the manuscript.

Acknowledgment—We thank A. M. Ball for excellent technical assistance.

References

1. Poger, D., and Mark, A. E. (2014) Activation of the epidermal growth factor receptor: a series of twists and turns. *Biochemistry* **53,** 2710–2721
2. Whorton, M. R., Bokoch, M. P., Rasmussen, S. G., Huang, B., Zare, R. N., Kobilka, B., and Sunahara, R. K. (2007) A monomeric G protein-coupled receptor isolated in a high-density lipoprotein particle efficiently activates its G protein. *Proc. Natl. Acad. Sci. U.S.A.* **104,** 7682–7687
3. Milligan, G. (2013) The prevalence, maintenance, and relevance of G protein-coupled receptor oligomerization. *Mol. Pharmacol.* **84,** 158–169
4. Pin, J. P., Comps-Agrar, L., Maurel, D., Monnier, C., Rives, M. L., Trinquet, E., Kniazeff, J., Rondard, P., and Prézeau, L. (2009) G-protein-coupled receptor oligomers: two or more for what? Lessons from mGlu and GABAB receptors. *J. Physiol.* **587,** 5337–5344
5. Calebiro, D., Rieken, F., Wagner, J., Sungkaworn, T., Zabel, U., Borzi, A., Cocucci, E., Zürn, A., and Lohse, M. J. (2013) Single-molecule analysis of fluorescently labeled G-protein-coupled receptors reveals complexes with distinct dynamics and organization. *Proc. Natl. Acad. Sci. U.S.A.* **110,** 743–748
6. Harikumar, K. G., Dong, M., and Miller, L. J. (2010) Secretin receptor dimerization: a possible functionally important paradigm for Family B GPCR dimerization in *GPCR Molecular Pharmacology and Drug Targetting: Shifting Paradigms and New Directions* (Gilchrist, A., ed) pp. 138–164, A. J. Wiley and Sons, Hoboken, NJ
7. Fiorentini, C., Gardoni, F., Spano, P., Di Luca, M., and Missale, C. (2003) Regulation of dopamine D1 receptor trafficking and desensitization by oligomerization with glutamate *N*-methyl-D-aspartate receptors. *J. Biol. Chem.* **278,** 20196–20202
8. Lee, L. T., Ng, S. Y., Chu, J. Y., Sekar, R., Harikumar, K. G., Miller, L. J., and Chow, B. K. (2014) Transmembrane peptides as unique tools to demonstrate the *in vivo* action of a cross-class GPCR heterocomplex. *FASEB J.* **28,** 2632–2644
9. Lee, V. H., Lee, L. T., Chu, J. Y., Lam, I. P., Siu, F. K., Vaudry, H., and Chow, B. K. (2010) An indispensable role of secretin in mediating the osmoregulatory functions of angiotensin II. *FASEB J.* **24,** 5024–5032
10. Chu, J. Y., Cheng, C. Y., Lee, V. H., Chan, Y. S., and Chow, B. K. (2011) Secretin and body fluid homeostasis. *Kidney Int.* **79,** 280–287
11. Chu, J. Y., Lee, L. T., Lai, C. H., Vaudry, H., Chan, Y. S., Yung, W. H., and Chow, B. K. (2009) Secretin as a neurohypophysial factor regulating body water homeostasis. *Proc. Natl. Acad. Sci. U.S.A.* **106,** 15961–15966
12. Chu, J. Y., Chung, S. C., Lam, A. K., Tam, S., Chung, S. K., and Chow, B. K. (2007) Phenotypes developed in secretin receptor-null mice indicated a role for secretin in regulating renal water reabsorption. *Mol. Cell. Biol.* **27,** 2499–2511
13. Lisenbee, C. S., and Miller, L. J. (2006) Secretin receptor oligomers form intracellularly during maturation through receptor core domains. *Biochemistry* **45,** 8216–8226
14. Harikumar, K. G., Morfis, M. M., Lisenbee, C. S., Sexton, P. M., and Miller, L. J. (2006) Constitutive formation of oligomeric complexes between family B G protein-coupled vasoactive intestinal polypeptide and secretin receptors. *Mol. Pharmacol.* **69,** 363–373
15. AbdAlla, S., Lother, H., and Quitterer, U. (2000) AT1-receptor heterodimers show enhanced G-protein activation and altered receptor sequestration. *Nature* **407,** 94–98
16. Cheng, Z. J., and Miller, L. J. (2001) Agonist-dependent dissociation of oligomeric complexes of G protein-coupled cholecystokinin receptors demonstrated in living cells using bioluminescence resonance energy transfer. *J. Biol. Chem.* **276,** 48040–48047
17. Lakowicz, J. R. (1999) Energy Transfer. in *Principles of Fluorescescence Spectroscopy*, 2nd Ed., pp. 367–394, Kluwer Academic/Plenum Publishers
18. Haas, E., Katchalski-Katzir, E., and Steinberg, I. Z. (1978) Effect of the orientation of donor and acceptor on the probability of energy transfer involving electronic transitions of mixed polarization. *Biochemistry* **17,** 5064–5070
19. Harikumar, K. G., Pinon, D. I., and Miller, L. J. (2007) Transmembrane segment IV contributes a functionally important interface for oligomerization of the Class II G protein-coupled secretin receptor. *J. Biol. Chem.* **282,** 30363–30372
20. Harikumar, K. G., Happs, R. M., and Miller, L. J. (2008) Dimerization in the absence of higher-order oligomerization of the G protein-coupled secretin receptor. *Biochim. Biophys. Acta* **1778,** 2555–2563
21. Gao, F., Harikumar, K. G., Dong, M., Lam, P. C., Sexton, P. M., Christopoulos, A., Bordner, A., Abagyan, R., and Miller, L. J. (2009) Functional importance of a structurally distinct homodimeric complex of the family B G protein-coupled secretin receptor. *Mol. Pharmacol.* **76,** 264–274
22. Garcia, G. L., Dong, M., and Miller, L. J. (2012) Differential determinants for coupling of distinct G proteins with the class B secretin receptor. *Am. J. Physiol. Cell Physiol.* **302,** C1202–C1212
23. Ulrich, C. D., 2nd, Pinon, D. I., Hadac, E. M., Holicky, E. L., Chang-Miller, A., Gates, L. K., and Miller, L. J. (1993) Intrinsic photoaffinity labeling of native and recombinant rat pancreatic secretin receptors. *Gastroenterology* **105,** 1534–1543
24. Chu, J. Y., Yung, W. H., and Chow, B. K. (2006) Endogenous release of secretin from the hypothalamus. *Ann. N.Y. Acad. Sci.* **1070,** 196–200
25. Daniels, D., and Marshall, A. (2012) Evaluating the potential for rostral diffusion in the cerebral ventricles using angiotensin II-induced drinking in rats. *Brain Res.* **1486,** 62–67
26. Hebert, T. E., Moffett, S., Morello, J. P., Loisel, T. P., Bichet, D. G., Barret, C., and Bouvier, M. (1996) A peptide derived from a β_2-adrenergic receptor transmembrane domain inhibits both receptor dimerization and activation. *J. Biol. Chem.* **271,** 16384–16392
27. Sauliere, A., Bellot, M., Paris, H., Denis, C., Finana, F., Hansen, J. T., Altie, M. F., Seguelas, M. H., Pathak, A., Hansen, J. L., Sénard, J. M., and Galés, C. (2012) Deciphering biased-agonism complexity reveals a new active AT1 receptor entity. *Nat. Chem. Biol.* **8,** 622–630
28. Hadac, E. M., Ghanekar, D. V., Holicky, E. L., Pinon, D. I., Dougherty, R. W., and Miller, L. J. (1996) Relationship between native and recombinant cholecystokinin receptors: role of differential glycosylation. *Pancreas* **13,** 130–139